View metadata, citation and similar papers at core.ac.uk
brought to you by CORE
provided by Institutional Repository of the Freie Universität Berlin

CONDENSED MATTER PHYSICS

Sensitivity of the superconducting state in thin films

I. Tamir[1,2]*, A. Benyamini[3], E. J. Telford[4], F. Gorniaczyk[1], A. Doron[1], T. Levinson[1], D. Wang[4], F. Gay[5], B. Sacépé[5], J. Hone[3], K. Watanabe[6], T. Taniguchi[6], C. R. Dean[4], A. N. Pasupathy[4], D. Shahar[1,4]

Copyright © 2019 The Authors, some rights reserved; exclusive licensee American Association for the Advancement of Science. No claim to original U.S. Government Works. Distributed under a Creative Commons Attribution NonCommercial License 4.0 (CC BY-NC).

For more than two decades, there have been reports on an unexpected metallic state separating the established superconducting and insulating phases of thin-film superconductors. To date, no theoretical explanation has been able to fully capture the existence of such a state for the large variety of superconductors exhibiting it. Here, we show that for two very different thin-film superconductors, amorphous indium oxide and a single crystal of 2H-$NbSe_2$, this metallic state can be eliminated by adequately filtering external radiation. Our results show that the appearance of temperature-independent, metallic-like transport at low temperatures is sufficiently described by the extreme sensitivity of these superconducting films to external perturbations. We relate this sensitivity to the theoretical observation that, in two dimensions, superconductivity is only marginally stable.

INTRODUCTION

All noninteracting two-dimensional (2D) electronic systems in the thermodynamic limit are expected to exhibit an insulating ground state (*1*). This prevailing notion has been challenged only in the case where strong interactions dominate the electronic state notably in low-disorder, strongly interacting semiconductors, where an apparent transition to metallic conduction at low temperatures (T's) has been observed (*2*, *3*).

The physics gets more complex in the case where electronic correlations can lead to superconductivity. It is theoretically accepted that, in realistic 2D systems, with the unavoidable disorder and at a finite T, superconductivity exists only marginally and finite resistivity is always expected (*4*, *5*). The value of this residual resistance is sensitive to the state of the system, and it usually depends exponentially on experimental variables such as T, magnetic field (B), measurement current (I), and the level of microscopic disorder. An exception is the case of exactly zero B, which can effectively be attained in experiments, where true superconductivity, with zero resistance at a finite T, is expected.

For these thin-film systems, the superconducting state can be markedly terminated with a transition to an insulating phase (*6*, *7*). In this superconductor-insulator transition (SIT), metallic behavior is expected to be restricted to an unstable point at the transition (*8*). This point of view is often supported by experiments using a variety of ways to drive the SIT including thickness variation, disorder, B, and carrier concentration [for a review, see (*9*)].

There is, however, a growing number of independent studies (*10*–*17*) where the observation of an unexpected metallic state, intervening between the superconducting and insulating phases, has been reported. The unique characteristic attributed to this "anomalous metal" is that the superconducting transition, signaled by an exponential decrease below a well-defined critical T, T_C, of the sheet resistance (R) from its normal state value, R_N, is terminated, upon further cooling, with a crossover to a T-independent R that persists down to the lowest T's. This behavior, seen in thin films for which R_N is substantially lower than the quantum of resistance $R_Q \equiv h/e^2 \simeq 25.8 k\Omega$, is observed over a wide range of experimental parameters and extends to relatively high T's (*18*). Unlike ordinary metals, this state exhibits a vanishing Hall effect that was associated with a new particle-hole symmetric ground state (*19*, *20*), its microwave response shows no cyclotron resonance, and it reveals the existence of short-range superconducting correlations (*21*).

The physical origin of this anomalous metallic state remains controversial, with experimental measurements variously interpreted as evidence of a Bose-metal phase (*16*) or dissipation arising from collective vortex tunneling (*10*, *15*). Although several theoretical groups have addressed this state (*19*, *22*–*31*), its robustness and ubiquitous nature pose difficulties in the development of a comprehensive model (*18*). The purpose of this article is to show that the apparent metallic behavior can result from an unforeseen sensitivity of these marginal superconductors to external perturbations.

RESULTS

Our data were obtained from two very different superconducting systems. The first is amorphous indium oxide (a:InO) thin film (Fig. 1, A and B), known for its high level of disorder reflected by high R_N ($\lesssim \frac{h}{4e^2} \simeq 6.4$ kilohms). The second system we investigated is made of sheets exfoliated from a single crystal of 2H-$NbSe_2$ (Fig. 1, C and D), which are of high purity and are characterized by low R_N (<100 ohms) (*32*). Within the field of thin-film superconductors, these two systems represent opposite limits with respect to structure and disorder. Moreover, while 2H-$NbSe_2$ is a purely 2D superconductor having a thickness $d \ll \xi$, ξ being the superconducting coherence length, d of the a:InO films is approximately five times larger than its ξ (*33*).

We begin by showing that the superconducting phase into which our samples transition at T_C, and which is interrupted as saturation sets in at lower T's, is completely restored by introducing external low-pass filters into the measurement setup (see fig. S1). This is illustrated by plotting R as a function of T^{-1} obtained from an a:InO film (Fig. 1E) and a 2H-$NbSe_2$ film (Fig. 1F). In both samples, R obtained from the unfiltered measurements (i.e., measured without additional external low-pass filters, red traces) initially decreased exponentially with an approximate activated behavior $R(T) \propto \exp(-U(B)/k_B T)$, where $U(B)$ is the activation energy and k_B is the Boltzmann constant. The exponential decrease then terminated with a transition to a saturated regime

[1]Department of Condensed Matter Physics, Weizmann Institute of Science, Rehovot 76100, Israel. [2]Fachbereich Physik, Freie Universität Berlin, 14195 Berlin, Germany. [3]Department of Mechanical Engineering, Columbia University, New York, NY 10027, USA. [4]Department of Physics, Columbia University, New York, NY 10027, USA. [5]University Grenoble Alpes, CNRS, Grenoble INP, Institut Néel, Grenoble 38000, France. [6]National Institute for Materials Science, 1-1 Namiki, Tsukuba 305-0044, Japan.
*Corresponding author. Email: idan.tamir@fu-berlin.de

Downloaded from http://advances.sciencemag.org/ on April 2, 2020

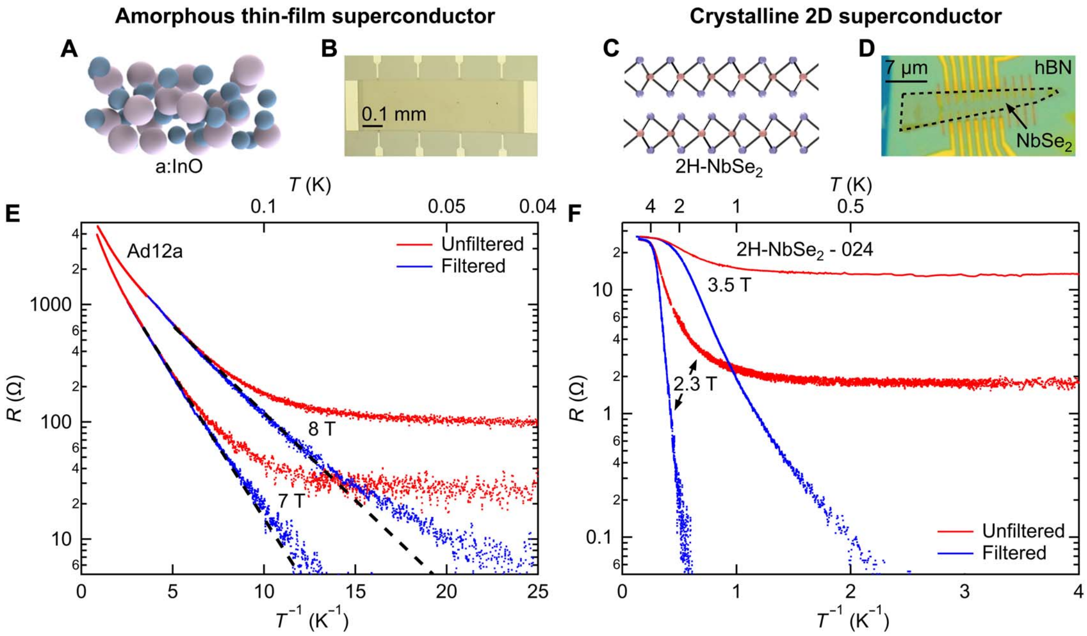

Fig. 1. Eliminating saturation. (**A** and **C**) System structure and (**B** and **D**) microscope image of a:InO (AD12a) and 2H-$NbSe_2$ (024) films, respectively. (**E** and **F**) R versus T^{-1} obtained from an a:InO film at B = 7 and 8 T, and a quad-layer 2H-$NbSe_2$ at B = 2.3 and 3.5 T, respectively. Blue traces are measured with, and red traces without, filters. The top axis indicates the corresponding T's. The black dashed lines in (E) are guides to the eye, indicating activated behavior. The data were measured by applying a standard four-terminal lock-in technique with I_0 = 1 (a:InO) and 100 (2H-$NbSe_2$) nA.

that persisted down to our lowest T's. It is this saturated behavior of R that was previously interpreted as indicating the novel metallic state (*10*, *15*, *16*, *18*).

When we repeated the measurements, this time with additional low-pass filters installed (blue traces), we found that R continued to follow the activated trend down to much lower T's, and as T was further lowered, R continued to decrease to our noise level without saturating. The external low-pass filters effectively reduce the bandwidth of our measurements from 1 to 30 MHz (set by the twisted pairs of resistive measurement wires acting as low-pass resistor–capacitor filters) down to 200 to 300 kHz, depending on the specific setup (see, e.g., fig. S2).The lowest R we now measure can exceed two orders of magnitude below the corresponding saturated values of the unfiltered measurements. We note that even with filtering, we continue to observe deviation from activated behavior in the lowest T ranges measured. However, we believe that this results from imperfect filters. Additional measurements of a:InO film in a second fridge with improved low-T filters show no deviation from activated behavior over the full range of achievable T's (Fig. 2). We conclude that our data do not support the existence of quantum corrections (*10*, *15*, *34*) to the well-known transport due to thermally activated vortices (*5*).

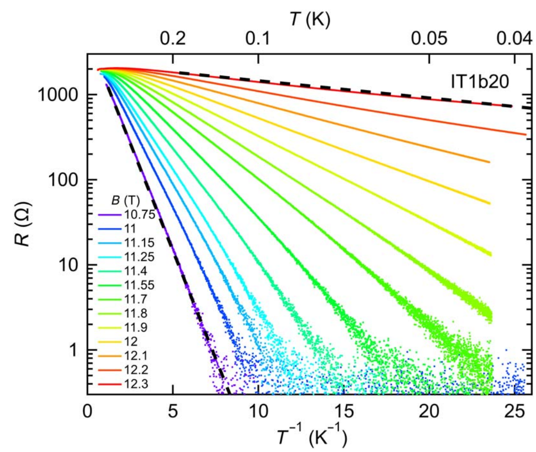

Fig. 2. Fully recovered activated behavior. R versus T^{-1} obtained from IT1b20, an a:InO film, measured with better filtration (see Materials and Methods for details) at different B values. Activated behavior (straight line in an Arrhenius plot) is apparent down to our noise floor or lowest measurement T's (see, e.g., dashed black lines at B = 10.75 and 12.3 T).

Although the effect the filters have on both systems is qualitatively similar, it is important to point out that, while for a:InO it is only seen well below T_C, for 2H-$NbSe_2$ filtering has a measurable effect right from T_C and at B = 0. In Fig. 3A, we show the thermodynamic superconducting-normal transitions of 2H-$NbSe_2$, at B = 0 in the left panel, and near H_{C_2} (the upper critical field terminating superconductivity) for several T's in the right. The common theme in these figures is that a significant effect of the filters is measured very close to the transition into superconductivity. In contrast, for a:InO, initial differences between filtered and unfiltered measurements are only seen much below T_C. This is summarized in Fig. 3B, where we present the $B - T$ phase diagram for our samples. For 2H-$NbSe_2$, the initial effect of the filters, indicated by green triangles, overlaps within error with the superconductor-normal phase boundary (defined by $R = 0.9 \cdot R_N$), while for a:InO the filters significantly influence the results only well within the superconducting phase, indicated by blue and red triangles.

While filtering external radiation effectively eliminates the apparent metallic behavior, we found that saturation can be reintroduced by increasing the current used in our four-terminal measurements. For this purpose, we used both DC and AC currents (I_{DC} and I_{AC}; see Materials and Methods) with similar results. The saturation induced

Downloaded from http://advances.sciencemag.org/ on April 2, 2020

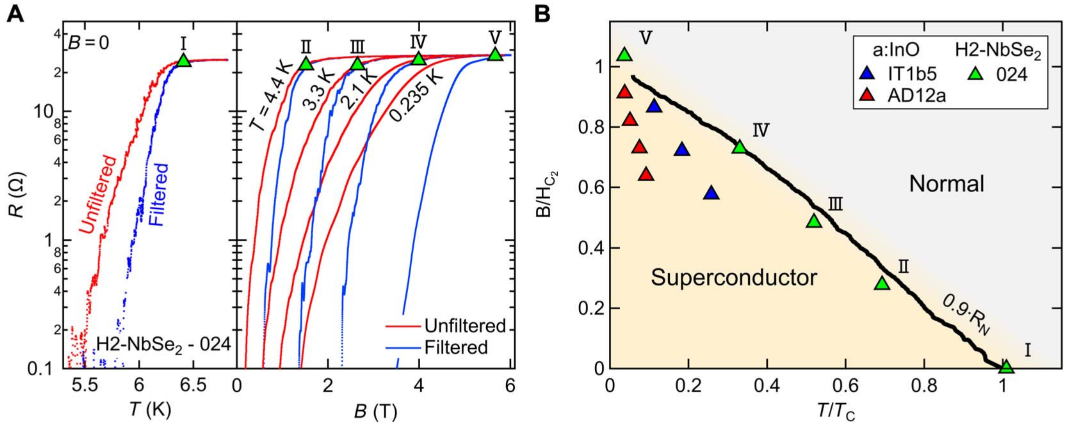

Fig. 3. Resistive transition. (**A**) Measurements of the T-driven (left) and B-driven (right) superconducting-normal phase transition in a 2H-NbSe2 film (024). Blue traces are measured with, and red traces without, filters. (**B**) B–T phase diagram. The black line separating the superconducting and normal phases, defined by $R = 0.9 \cdot R_N$, is obtained from the 2H-NbSe2 sample and includes data that were left out from (A) for visibility. The T and B values, where $\Delta R/R_F = (R_{Unfiltered} - R_{Filtered})/R_{Filtered} = 3\%$, are marked in both (A) and (B) by green triangles. Both T_C and H_{C_2} are defined at $R = 0.9 \cdot R_N$. For our a:InO films, blue and red triangles, we used $T_C = 2.5$ K (Ad12a) and 3 K (IT1b5).

by increasing I_{AC} is demonstrated in Fig. 4A, where we present data obtained from an a:InO film measured with filters at $B = 10$ T, using increasing levels of I_0 (the amplitude of I_{AC}). While at $I_0 = 1$ nA, the measured V/I, where V is the voltage drop along the sample, followed an activated behavior with deviations that are barely noticeable over our noise level, for $I_0 \geq 50$ nA the data significantly deviated from its low-I_0 value and saturation set-in at low T's, with the saturated value increasing with I_0. For reference, we include one trace (red) measured without filters and at $I_0 = 1$ nA, which exhibits the low-T saturation. We note that, because R is an equilibrium value defined by $\lim_{I \to 0} V/I$, the data presented in Fig. 4A strictly equal R only in the ohmic regime ($I_0 \lesssim 1$ nA). Similar results are obtained while increasing I_{DC} (see Fig. 4B, where we present data obtained from a 2H-NbSe$_2$ film).

When superconductors are subjected to strong enough B, their transport properties are dominated by vortex physics (*5*). Excessive I can dislodge vortices, which are otherwise pinned at low T's, inducing voltage and dissipation. The saturation induced in our experiment by increasing I can therefore be attributed to heating. Under the application of a higher power ($P = I \cdot V$) by the measurement circuit, the electronic system is unable to equilibrate with its low-T environment. This leads to an out-of-equilibrium steady state where the electrons are held at an elevated T, T_{eff}, higher than the surrounding T (*35*). The I-induced deviations from activated behavior, as well as the saturation regions, can therefore be attributed to $T_{eff} > T$. We can self-consistently extract these T_{eff}'s by fitting the $R(T)$ data, obtained from the filtered measurements in the ohmic regime, with an activated form and then using this fit as our thermometry calibration curve: For each value of V/I, in the elevated I measurements, we associate a T_{eff} corresponding to $V/I = R$ in the calibration curve. Using this procedure, we conveniently define T_{sat} as T_{eff} in the R saturation regime.

We now wish to suggest that the R saturation observed in our unfiltered experiments, and which bears a notable resemblance to the I-driven saturation (see Fig. 4A), can also be associated with heating. While in this case the source of heating is less obvious, the fact that filtering the electrical lines connected to the sample effectively eliminates the saturation suggests that the culprit is ambient noise currents that propagate down the lines and couple directly to the low-T electronic system. We can estimate the power density (p) delivered to the electronic system by these noise currents (p_r) by comparing T_{sat} obtained during the application of known p in our filtered, elevated I measurements (T^I_{sat}) to the T_{sat} obtained in the unfiltered, ohmic measurements (T^r_{sat}). To do this, we plot, in Fig. 4C, the p dependence of T^I_{sat} for two of our samples and use it as our p meter. Red diamonds indicate T^r_{sat} values corresponding to the unfiltered curves of each sample. We find $p_r = 1.8$ W/cm^3 for the a:InO sample and 8.2×10^4 W/cm^3 for the 2H-NbSe$_2$ sample.

Although our results show that our a:InO and 2H-NbSe$_2$ films do not exhibit an intermediate metallic phase, we cannot rule out the existence of such a phase in other superconducting systems for which a metallic state was previously reported (*10*, *15*). We can, however, naively extend our effective-temperature analysis to these systems. In Fig. 4D, we present T_{sat} versus B obtained from our data (blue and green symbols), together with T_{sat} values that we extracted from published data (black symbols). Whenever comparisons between results obtained from filtered and unfiltered measurements are not available (empty symbols), we fitted the data measured at higher T's with activated behavior and used these fits as our thermometry calibration curves. This procedure, introduced in this context in (*10*), only provides a lower bound for T_{sat} because the filtered measurements can also exhibit higher $U(B)$ (see fig. S3). While the data in Fig. 4D represent several very different systems, measured over a wide range of T's, they all share a similar B dependence: We found that $T_{sat} \sim \log(H_{C_2}/\alpha B)$, where α is a fit parameter of order 1, works reasonably well.

Before we proceed to discuss the implication of this simple elevated effective-temperature scenario, we wish to point out that there are other possible mechanisms that would lead to I-dependent transport in thin-film superconductor such as ours. Nonlinear vortex–related response may be relevant at finite B's, and Berezinskii–Kosterlitz–Thouless vortex-antivortex unbinding may be at work at $B = 0$. At this stage, we are unable to rule out that these mechanisms play a notable role in the I response of the system and may even lead to saturated, T-independent R as $T \to 0$. We are not aware of a model that accounts for the stark difference between the results of the filtered and unfiltered measurements.

DISCUSSION

The data we present here show that the metallic behavior, often observed in thin-film superconductors, results from the exposure of the

Downloaded from http://advances.sciencemag.org/ on April 2, 2020

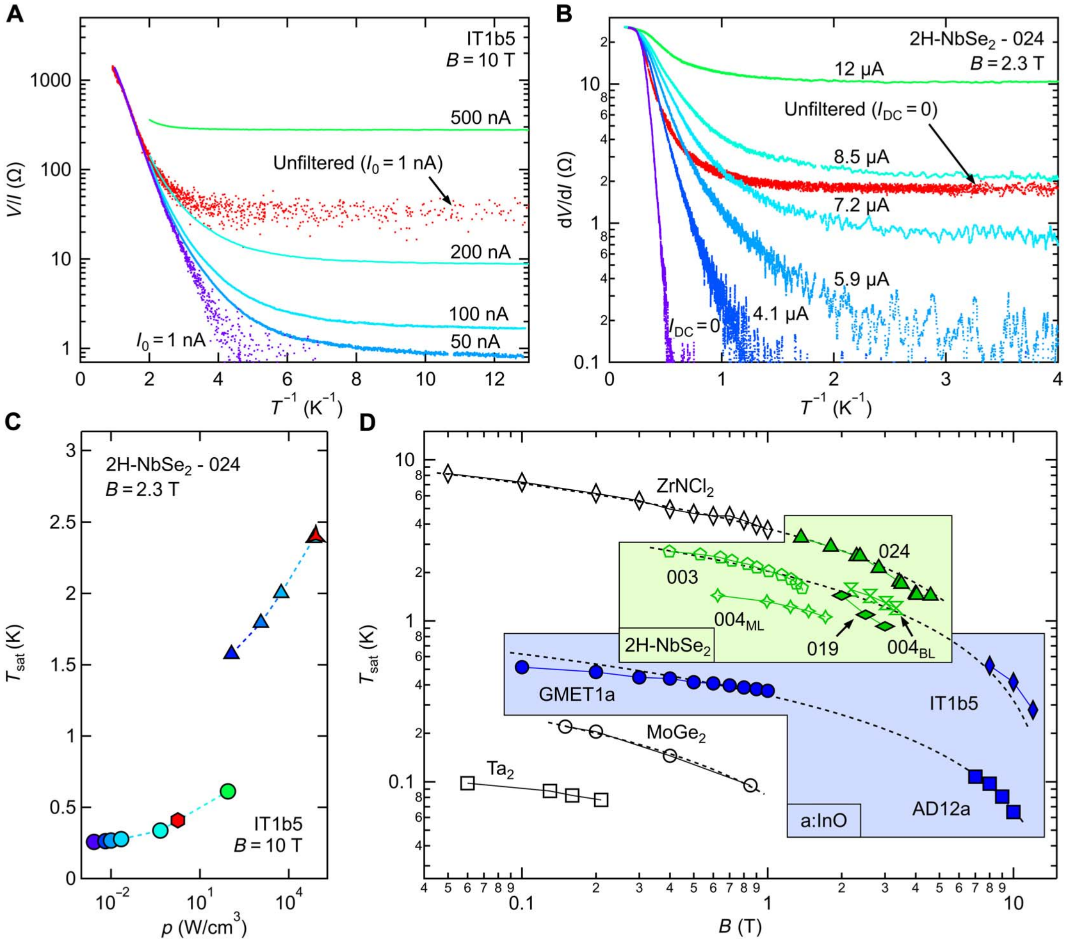

Fig. 4. Induced saturation and saturation *T*. (**A**) *V*/*I* versus T^{-1} obtained from an a:InO film, measured at *B* = 10 T with increasing I_0's. (**B**) d*V*/d*I* versus T^{-1} obtained from a 2H-NbSe2 film, measured at *B* = 2.3 T with an increasing level of I_{DC} (see Materials and Methods). In both (A) and (B), we include one trace (red) measured, at our lowest *I*, without filters. (**C**) T^{I}_{sat} versus *p* extracted from the a:InO data presented in (A) (circles), and the 2H-NbSe2 data presented in (B) (triangles), adopting the same color scale for the different *I*'s. The red symbols represent T^{r}_{sat} extracted from the unfiltered measurements. The a:InO data include I_{AC}'s left out of (A) for visibility. These curves are used as *p* meters to estimate p_r = 1.8 and 8.2 × 10^4 W/cm^3 for the a:InO and 2H-NbSe2 samples, respectively. (**D**) T_{sat} versus *B* evaluated for several samples. Our data are plotted in blue (a:InO) and green (2H-NbSe$_2$). The MoGe (*10*), Ta (*11*), and ZrNCl (*15*) data (black symbols) were extracted from the cited references. Full symbols represent data that were calculated using filtered measurements as a thermometer, while data plotted with empty symbols were estimated following the procedure in (*10*). All samples exhibit similar logarithmic *B* dependence (see dashed black lines).

Downloaded from http://advances.sciencemag.org/ on April 2, 2020

superconducting phase to unwanted radiation or high *I*'s. While these can, in many cases, be eliminated, it is still worthwhile to consider why these superconductors so readily respond to excitations that leave other systems, under similar conditions (see the Supplementary Materials for further discussion), unaffected. We point out that T_{sat} is routinely around a few kelvin, where it is unlikely that the cryogenic environment will limit the sample's ability to cool. Because the external power couples only to the electronic system, which exhibits an exponential *T* dependence, it is reasonable to conclude that the observed sensitivity is a result of a bottleneck in the heat-transfer process that is between the electrons and the host phonons (*35*). This is not unexpected because in superconductors the electron condensate is decoupled from the heat-carrying phonons. If such a limiting mechanism is at play, a much more thorough theoretical analysis is necessary before we can go any further with quantitative tests.

In this study, we were able to compare two very different systems under virtually identical measurement conditions. It is reasonable to assume that, without filters, the radiation delivered to both types of samples would be the same. Unexpectedly, we find very different p_r's. Similarly, their T_{sat} values are different: <0.4 K for a:InO and ~2 K for 2H-NbSe$_2$. If the effective-temperature picture is correct, we need to understand why two samples under similar external radiation end up responding in such a different manner. The reason, we believe, is rooted in the energy balance maintained by the electrons. Even if the radiation is the same, it is very likely that different systems will absorb this energy in different ways, reflecting the specific details of their electronic state. Compounding this are possible differences between the strength of the coupling to the phonon system to which the electrons can transfer the energy absorbed from the radiation. A detailed understanding of this scenario awaits further theoretical developments.

In summary, we showed that two very different thin-film superconductors are extremely sensitive to external perturbations and, in response to such perturbations, exhibit metallic-like, saturated *T* dependence. We suggested two possible mechanisms: The first is based on vortex depinning, and in the other, we assume that an overheated state exists, where the electronic system is unable to equilibrate with its surroundings. In the latter case, one should theoretically address not only the external power dissipated but also the heat flow away from the electronic system.

MATERIALS AND METHODS

In this work, we studied several different a:InO and 2H-$NbSe_2$ samples. Their relevant parameters are presented in table S1. Details of the growth and fabrication were previously published [see (*32*) for 2H-$NbSe_2$ and (*36*) for a:InO].

The data presented in Fig. 2 were measured in a dilution refrigerator equipped with heavily filtered DC lines comprising feedthrough pi filters at room temperature, low-resistance twisted pairs (~8 ohms) from 300 to 4 K to reduce Johnson noise, lossy shielded twisted-pairs (~500 ohms) from 4 K to the mixing chamber (MC) stage, copper-powder filter (*37*) on the MC stage, and cryogenic-compatible 47-nF capacitor-to-ground on the sample holder. Furthermore, as thermometry below 0.1 K is delicate, a RuO_2 thermometer calibrated by 60Co nuclear orientation thermometry has been installed on the sample holder close to the sample; thus, it was subjected to the same cooling power from the wiring. This additional on-chip thermometry suppresses the very last deviations from activated transport at the lowest T's.

SUPPLEMENTARY MATERIALS

Supplementary material for this article is available at http://advances.sciencemag.org/cgi/content/full/5/3/eaau3826/DC1

Fig. S1. Schematics of the measurement circuit.
Fig. S2. Probe transmission.
Fig. S3. Activation energy.
Table S1. Sample parameters.
References (*38–40*)

REFERENCES AND NOTES

1. E. Abrahams, P. W. Anderson, D. C. Licciardello, T. V. Ramakrishnan, Scaling theory of localization: Absence of quantum diffusion in two dimensions. *Phys. Rev. Lett.* **42**, 673–676 (1979).
2. S. V. Kravchenko, G. V. Kravchenko, J. E. Furneaux, V. M. Pudalov, M. D'Iorio, Possible metal-insulator transition at *B*=0 in two dimensions. *Phys. Rev. B* **50**, 8039–8042 (1994).
3. A. Punnoose, A. M. Finkel'stein, Metal-insulator transition in disordered two-dimensional electron systems. *Science* **310**, 289–291 (2005).
4. M. P. A. Fisher, Quantum phase transitions in disordered two-dimensional superconductors. *Phys. Rev. Lett.* **65**, 923–926 (1990).
5. M. Feigel'man, V. B. Geshkenbein, A. I. Larkin, Pinning and creep in layered superconductors. *Phys. C Supercond.* **167**, 177–187 (1990).
6. D. B. Haviland, Y. Liu, A. M. Goldman, Onset of superconductivity in the two-dimensional limit. *Phys. Rev. Lett.* **62**, 2180–2183 (1989).
7. A. F. Hebard, M. A. Paalanen, Magnetic-field-tuned superconductor-insulator transition in two-dimensional films. *Phys. Rev. Lett.* **65**, 927–930 (1990).
8. S. L. Sondhi, S. M. Girvin, J. P. Carini, D. Shahar, Continuous quantum phase transitions. *Rev. Mod. Phys.* **69**, 315–333 (1997).
9. V. F. Gantmakher, V. T. Dolgopolov, Superconductor–insulator quantum phase transition. *Phys.-Uspekhi* **53**, 1–49 (2010).
10. D. Ephron, A. Yazdani, A. Kapitulnik, M. R. Beasley, Observation of quantum dissipation in the vortex state of a highly disordered superconducting thin film. *Phys. Rev. Lett.* **76**, 1529–1532 (1996).
11. Y. Qin, C. L. Vicente, J. Yoon, Magnetically induced metallic phase in superconducting tantalum films. *Phys. Rev. B* **73**, 100505 (2006).
12. O. Crauste, C. A. Marrache-Kikuchi, L. Bergé, D. Stanescu, L. Dumoulin, Thickness dependence of the superconductivity in thin disordered NbSi films. *J. Phys. Conf. Ser.* **150**, 042019 (2009).
13. J. T. Ye, Y. J. Zhang, R. Akashi, M. S. Bahramy, R. Arita, Y. Iwasa, Superconducting dome in a gate-tuned band insulator. *Science* **338**, 1193–1196 (2012).
14. J. Garcia-Barriocanal, A. Kobrinskii, X. Leng, J. Kinney, B. Yang, S. Snyder, A. M. Goldman, Electronically driven superconductor-insulator transition in electrostatically doped $La_2CuO_{4+\delta}$ thin films. *Phys. Rev. B* **87**, 024509 (2013).
15. Y. Saito, Y. Kasahara, J. Ye, Y. Iwasa, T. Nojima, Metallic ground state in an ion-gated two-dimensional superconductor. *Science* **350**, 409–413 (2015).
16. A. W. Tsen, B. Hunt, Y. D. Kim, Z. J. Yuan, S. Jia, R. J. Cava, J. Hone, P. Kim, C. R. Dean, A. N. Pasupathy, Nature of the quantum metal in a two-dimensional crystalline superconductor. *Nat. Phys.* **12**, 208–212 (2016).
17. Y. Saito, T. Nojima, Y. Iwasa, Quantum phase transitions in highly crystalline two-dimensional superconductors. *Nat. Commun.* **9**, 778 (2018).
18. A. Kapitulnik, S. A. Kivelson, B. Spivak, Anomalous metals—Failed superconductors. arXiv:1712.07215 [cond-mat.supr-con] (19 December 2017).
19. M. Mulligan, S. Raghu, Composite fermions and the field-tuned superconductor-insulator transition. *Phys. Rev. B* **93**, 205116 (2016).
20. N. P. Breznay, A. Kapitulnik, Particle-hole symmetry reveals failed superconductivity in the metallic phase of two-dimensional superconducting films. *Sci. Adv.* **3**, e1700612 (2017).
21. Y. Wang, I. Tamir, D. Shahar, N. P. Armitage, Absence of cyclotron resonance in the anomalous metallic phase in InO_x. *Phys. Rev. Lett.* **120**, 167002 (2018).
22. D. Stauffer, A. Aharony, *Introduction to Percolation Theory* (CRC Press, 1994).
23. E. Shimshoni, A. Auerbach, A. Kapitulnik, Transport through quantum melts. *Phys. Rev. Lett.* **80**, 3352–3355 (1998).
24. D. Das, S. Doniach, Existence of a Bose metal at $T = 0$. *Phys. Rev. B* **60**, 1261–1275 (1999).
25. A. Kapitulnik, N. Mason, S. A. Kivelson, S. Chakravarty, Effects of dissipation on quantum phase transitions. *Phys. Rev. B* **63**, 125322 (2001).
26. P. Phillips, D. Dalidovich, The elusive bose metal. *Science* **302**, 243–247 (2003).
27. A. Larkin, A. Varlamov, *Theory of Fluctuations in Superconductors* (Clarendon Press, 2005).
28. V. M. Galitski, G. Refael, M. P. A. Fisher, T. Senthil, Vortices and quasiparticles near the superconductor-insulator transition in thin films. *Phys. Rev. Lett.* **95**, 077002 (2005).
29. B. Spivak, P. Oreto, S. A. Kivelson, Theory of quantum metal to superconductor transitions in highly conducting systems. *Phys. Rev. B* **77**, 214523 (2008).
30. S. Raghu, G. Torroba, H. Wang, Metallic quantum critical points with finite BCS couplings. *Phys. Rev. B* **92**, 205104 (2015).
31. M. Mulligan, Particle-vortex symmetric liquid. *Phys. Rev. B* **95**, 045118 (2017).
32. E. Telford, A. Benyamini, D. Rhodes, D. Wang, Y. Jung, A. Zangiabadi, K. Watanabe, T. Taniguchi, S. Jia, K. Barmak, A. N. Pasupathy, C. R. Dean, J. Hone, Via method for lithography free contact and preservation of 2d materials. *Nano Lett.* **18**, 1416–1420 (2018).
33. B. Sacépé, J. Seidemann, M. Ovadia, I. Tamir, D. Shahar, C. Chapelier, C. Strunk, B. A. Piot, High-field termination of a Cooper-pair insulator. *Phys. Rev. B* **91**, 220508 (2015).
34. I. M. Percher, I. Volotsenko, A. Frydman, B. I. Shklovskii, A. M. Goldman, Vortex variable range hopping in a conventional superconducting film. *Phys. Rev. B* **96**, 224511 (2017).
35. B. L. Altshuler, V. E. Kravtsov, I. V. Lerner, I. L. Aleiner, Jumps in current-voltage characteristics in disordered films. *Phys. Rev. Lett.* **102**, 176803 (2009).
36. D. Shahar, Z. Ovadyahu, Superconductivity near the mobility edge. *Phys. Rev. B* **46**, 10917–10922 (1992).
37. J. M. Martinis, M. H. Devoret, J. Clarke, Experimental tests for the quantum behavior of a macroscopic degree of freedom: The phase difference across a Josephson junction. *Phys. Rev. B* **35**, 4682–4698 (1987).
38. M. L. Roukes, M. R. Freeman, R. S. Germain, R. C. Richardson, M. B. Ketchen, Hot electrons and energy transport in metals at millikelvin temperatures. *Phys. Rev. Lett.* **55**, 422–425 (1985).
39. M. E. Gershenson, D. Gong, T. Sato, B. Karasik, A. Sergeev, Millisecond electron–phonon relaxation in ultrathin disordered metal films at millikelvin temperatures. *Appl. Phys. Lett.* **79**, 2049–2051 (2001).
40. F. C. Wellstood, C. Urbina, J. Clarke, Hot-electron effects in metals. *Phys. Rev. B* **49**, 5942–5955 (1994).

Acknowledgments: We are grateful to I. Aleiner, B. Altshuler, M. Feigelman, D. Kennes, S. A. Kivelson, K. Michaeli, A. Millis, P. W. Phillips, and B. Spivak for fruitful discussions. **Funding:** This research was supported by The Israel Science Foundation (ISF grant no. 556/17), the Minerva Foundation, Federal German Ministry for Education and Research, Grant No. 712942, the Horizon 2020 European Research Council (ERC) grant QUEST no. 637815, the NSF MRSEC program through Columbia in the Center for Precision Assembly of Superstratic and Superatomic Solids (DMR-1420634), the Global Research Laboratory (GRL) Program

Downloaded from http://advances.sciencemag.org/ on April 2, 2020

(2016K1A1A2912707) funded by the Ministry of Science, ICT and Future Planning via the National Research Foundation of Korea (NRF), and Honda Research Institute USA Inc. A portion of this work was performed at the National High Magnetic Field Laboratory, which is supported by National Science Foundation Cooperative Agreement Nos. DMR-1157490 and DMR-1644779 and the State of Florida. We also acknowledge the support provided by The Leona M. and Harry B. Helmsley Charitable Trust. **Author contributions:** I.T., A.B., E.J.T., F. Gorniaczyk, A.D., T.L., K.W., and T.T. prepared the samples. I.T., A.B., E.J.T., F. Gorniaczyk, A.D., T.L., D.W., F. Gay, and B.S. performed the experiments. I.T. and A.B. carried out the analysis and interpretation of the results. I.T. wrote the manuscript with the input of all co-authors. B.S., J.H., C.R.D., A.N.P., and D.S. supervised the project. **Competing interests:** The authors declare that they have no competing interests. **Data and materials availability:** All data needed to evaluate the conclusions in the paper are present in the paper and/or the Supplementary Materials. Additional data related to this paper may be requested from the authors.

Submitted 5 June 2018
Accepted 30 January 2019
Published 15 March 2019
10.1126/sciadv.aau3826

Citation: I. Tamir, A. Benyamini, E. J. Telford, F. Gorniaczyk, A. Doron, T. Levinson, D. Wang, F. Gay, B. Sacépé, J. Hone, K. Watanabe, T. Taniguchi, C. R. Dean, A. N. Pasupathy, D. Shahar, Sensitivity of the superconducting state in thin films. *Sci. Adv.* **5**, eaau3826 (2019).

Downloaded from http://advances.sciencemag.org/ on April 2, 2020

Science Advances

Sensitivity of the superconducting state in thin films

I. Tamir, A. Benyamini, E. J. Telford, F. Gorniaczyk, A. Doron, T. Levinson, D. Wang, F. Gay, B. Sacépé, J. Hone, K. Watanabe, T. Taniguchi, C. R. Dean, A. N. Pasupathy and D. Shahar

Sci Adv **5** (3), eaau3826.
DOI: 10.1126/sciadv.aau3826

ARTICLE TOOLS http://advances.sciencemag.org/content/5/3/eaau3826

SUPPLEMENTARY MATERIALS http://advances.sciencemag.org/content/suppl/2019/03/11/5.3.eaau3826.DC1

REFERENCES This article cites 37 articles, 4 of which you can access for free
http://advances.sciencemag.org/content/5/3/eaau3826#BIBL

PERMISSIONS http://www.sciencemag.org/help/reprints-and-permissions

Downloaded from http://advances.sciencemag.org/ on April 2, 2020

Use of this article is subject to the Terms of Service

Science Advances (ISSN 2375-2548) is published by the American Association for the Advancement of Science, 1200 New York Avenue NW, Washington, DC 20005. The title *Science Advances* is a registered trademark of AAAS.

Copyright © 2019 The Authors, some rights reserved; exclusive licensee American Association for the Advancement of Science. No claim to original U.S. Government Works. Distributed under a Creative Commons Attribution NonCommercial License 4.0 (CC BY-NC).